Experimental Performance Evaluation of Outdoor TDoA and RSS Positioning in a Public LoRa Network

D. Plets, N. Podevijn, J. Trogh, L. Martens, W. Joseph
Information Technology Department, imec-Ghent University
Technologiepark 15, B-9052 Ghent, Belgium
david.plets@ugent.be

***Abstract*—This paper experimentally compares the positioning accuracy of TDoA-based and RSS-based localization in a public outdoor LoRa network in the Netherlands. The performance of different Received Signal Strength (RSS)-based approaches (proximity, centroid, map matching,...) is compared with Time-Difference-of-Arrival (TDoA) performance. The number of RSS and TDoA location updates and the positioning accuracy per spreading factor (SF) is assessed, allowing to select the optimal SF choice for the network. A road mapping filter is applied to the raw location estimates for the best algorithms and SFs. RSS-based approaches have median and maximal errors that are limited to 1000 m and 2000 m respectively, using a road mapping filter. Using the same filter, TDoA-based approaches deliver median and maximal errors in the order of 150 m and 350 m respectively. However, the number of location updates per time unit using SF7 is around 10 times higher for RSS algorithms than for the TDoA algorithm.**

I. Introduction

Internet-of-Things (IoT) systems have tried to connect small devices to the internet, with the purpose of collecting relevant sensor data at known locations (e.g., smart electricity meters, smart parking, forest fire detection...). However, when the sensor is mobile (e.g., air quality sensor on a postal car), it is required to also know the approximate location of the measurement. In other cases, the location is even the only parameter of interest (e.g., fleet or goods tracking). Location tracking in outdoor environments is traditionally done via Global Positioning Systems (GPS), calculating the location with an accuracy of around 5 m. When this location also has to be known in a central backend system, the calculated GPS position is typically transmitted over an IoT network. The feasibility of using LoRa to transmit information (such as e.g., a GPS location) from a mobile node is addressed in [1] and has been applied and documented in several papers [2]–[6]. However, as GPS requires energy-intensive calculations on the mobile receiver, this technique puts an additional burden on energy-constrained devices. In a LoRa network, an alternative and more energy-efficient solution is to perform localization, only based on the LoRa messages that are transmitted by the mobile device, by applying TDoA techniques on the backend side. However, this approach has expected positioning accuracies that are worse compared to GPS, and moreover, it requires time-synchronized LoRa base stations (BS). LoRa localization, either via TDoA or via RSS techniques, has been given very limited attention in the research community so far. In [7], TDoA-based positioning was performed at three static locations, with an achieved accuracy of around 100 m. The most extensive TDoA performance assessment so far was presented in [8], where the number of location updates and positioning accuracy was determined for three mobility profiles ('walking', 'cycling', and 'driving'), and for all six SFs. In case the BSs are not time-synced, the backend system can rely on Received Signal Strength (RSS) techniques to estimate the location of the mobile device, but expected accuracies are lower than for TDoA. In [9], LoRa RSS-based localization experiments were presented, but in a relatively small, controlled, and hence, unrealistic environment. In [10], RSS localization has been investigated experimentally for Sigfox, another IoT technology. Table I provides a comparison of different LoRa-based positioning approaches. In this paper, we will for the first time assess the RSS positioning performance in a realistic LoRa network, for different spreading factors (SFs), and make the comparison with LoRa TDoA performance. This work will build on the same data set that was collected in [8]. The feasibility of applying a road mapping filter to improve the performance of either of the aforementioned systems will be investigated. The work will allow assessing to what extent these approaches are suited for applications where GPS has a too large impact on the energy lifetime of the tracked node to warrant TDoA calculations on the mobile node.

The outline of this paper is as follows. Section II describes the measurement configuration and Section III presents the localization algorithms. In Section IV, the results are discussed and the main findings of this paper are summarized in Section V.

TABLE I
Comparison of different LoRa-based approaches to perform outdoor localization.

	LoRa backend complexity	mobile node energy consumption	expected accuracy
GPS-over-LoRa	✓	X	✓✓
LoRa TDoA	X	✓	✓
LoRa RSS	✓	✓	X

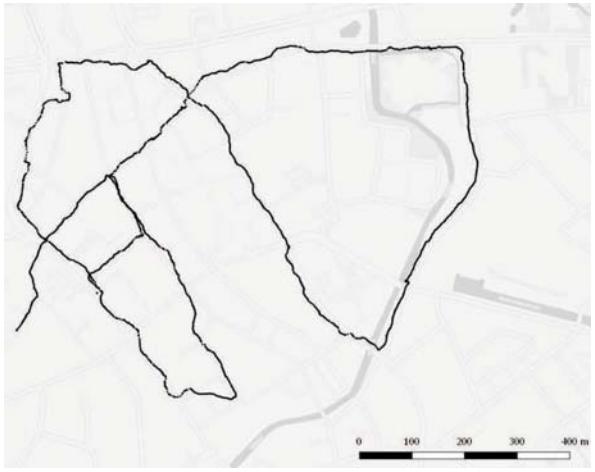

Fig. 1. Walking route with indication of LoRa base stations (triangles)

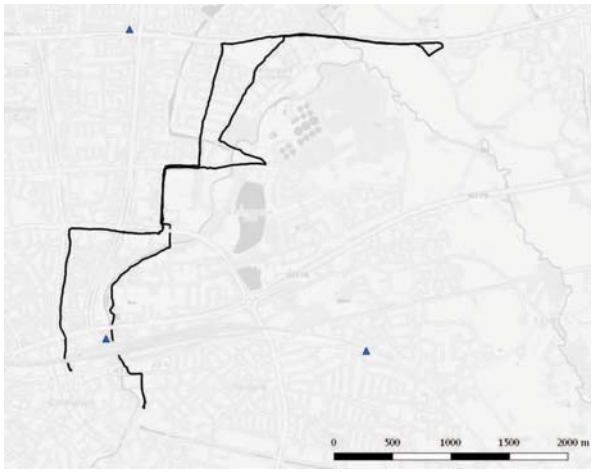

Fig. 2. Cycling route with indication of LoRa base stations (triangles)

II. Measurement configuration

The experiments are executed in a public LoRa network in and around Eindhoven, a (sub)urban city in the Netherlands. Six LoRa nodes with respective spreading factors between 7 and 12 were configured and provisioned, with Adaptive Data Rate (ADR) disabled to maintain a fixed spreading factor. These six LoRa SFs correspond to orthogonal spread signals at the same frequency, but with chirp durations that are specific per SFs: SF7 has the shortest time on air and the highest bit rate, SF12 has the longest time on air and the lowest bit rate. Messages are being sent with a size of 2 bytes, allowing transmission of e.g., battery level and sensor data. The application server recorded the JSON messages from the network server. For each device, it contains timestamps with the raw TDoA location estimates (in latitude and longitude degrees) and the Estimated Signal Power (ESP) values observed at the base stations for which the mobile device is within coverage range. Similarly to RSS reports, the ESP value is a measure of the received signal power, but excludes the noise power from its value. Although solely working with ESP values in this paper, we refer to the algorithms as 'RSS-based' algorithms, for ease of understanding.

The six mobile nodes with respective SFs between 7 and 12 were carried along 3 different routes: walking, cycling and driving: see Figs. 1, 2, 3. The ground truth (with timestamp) of each trajectory was recorded using a GPS logger with an update rate of 1 Hz. The characteristics of the three trajectories such as average speed, maximum speed, travelled distance and duration are summarized in Table II.

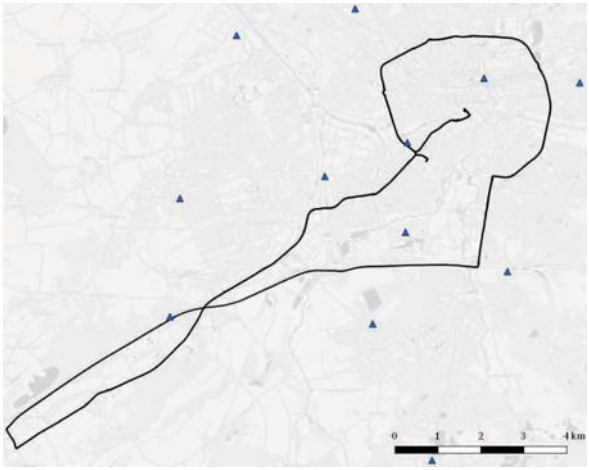

Fig. 3. Driving route with indication of LoRa base stations (triangles)

TABLE II
Characteristics of the three one-hour long trajectories

	Total distance	Average speed	Maximum speed
Walking	4.4 km	4.4 km/h	6 km/h
Cycling	12.1 km	12.1 km/h	21 km/h
Driving	38.7 km	38.7 km/h	137 km/h

Based on the messages from the network server, the algorithms presented in Section III calculate an estimated position of the mobile device, for each trajectory and SF. Using the timestamps of the GPS logger and the server messages, the positioning errors were calculated for each combination of node (each SF) and each trajectory.

III. Algorithms

This section will present the set of algorithms that will be used to estimate the location of the mobile nodes. Fig. 4 shows that in a first step, raw location estimates are calculated based on an RSS or TDoA approach. In a second step, a road mapping filter is applied to these estimates to further improve their accuracy.

A. Raw location estimation algorithms

In the first subsection, five algorithms delivering raw location estimates will be described.

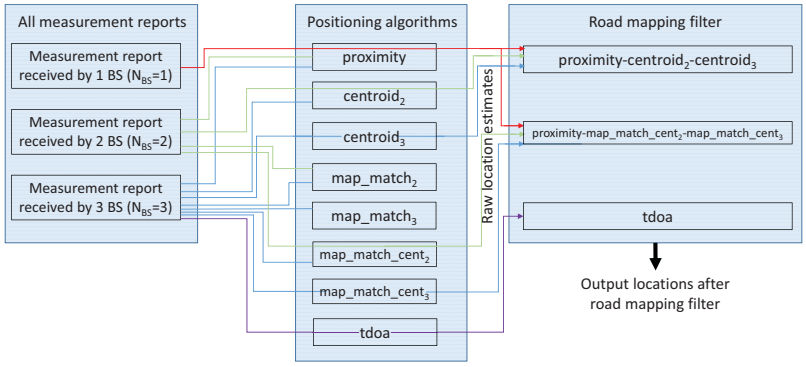

Fig. 4. Overview of how original measurement data is used in the different algorithms and how raw location estimated are used in the road mapping filters.

1) TDoA: TDoA localization (denoted as $tdoa$ hereafter) is based on measurements of the time difference between Time-of-Arrival measurements at different BSs. This algorithm is well-known and is described in e.g., [11]. Due to the lower bandwidth of the LoRa signal compared to GPS, timing information is less accurate and positioning accuracies are worse. A TDoA position calculation requires a measurement report to be received at three or more time-synced LoRa BSs.

2) RSS proximity: The proximity algorithm is based on RSS values, by estimating the node location as that of the BS that receives the strongest signal from the mobile node. This BS is assumed to be located closest to the node. Unlike for traditional localization algorithms requiring three BSs within range of the node, this approach only requires only one BS within range. However, expected positioning errors are larger.

3) RSS centroid: The centroid localization algorithm maps the estimated location to the center of the two or three BSs that receive the strongest signal from the mobile node. In case only the two strongest received signals are considered, the estimated location corresponds to the middle of the line segment formed by the two BSs that receive the signal (denoted as $centroid_2$ hereafter). If three BSs receive the signal, the location is estimated at the center of the triangle formed by the three BSs (denoted as $centroid_3$ hereafter). In general, this approach is more accurate than the one mapping the location to the closest BS, but it requires two or three BSs within the range of the mobile node, so fewer location updates are expected.

4) RSS map matching: The RSS map matching approach is based on finding the location for which the set of *measured* RSS values at the BSs form the best fit with the RSS values that are *predicted* based on a path loss model. This fitness of each candidate location L is determined by the following cost function C_L:

$$C_L = \sum_{i}^{N_{BS}} (ESP_{meas}^{BSi} - ESP_{est,L}^{BSi})^2, \qquad (1)$$

with ESP_{meas}^{BSi} the ESP value measured at base station BSi, $ESP_{est,L}^{BSi}$ the ESP that is estimated to be received at location L, and N_{BS} the number of BSs that receive the signal. The estimated location L', is the location for which C_L is the lowest, after evaluating all possible locations L. $ESP_{est,L}^{BSi}$ will be modeled according to a one-slope log-distance relation [12]:

$$ESP_{est,L}^{BSi} = ESP_{100} - 10n \cdot log(d_{BSi}^{L}/100), \qquad (2)$$

with ESP_{100} [dB] the ESP value recorded with the node at 100 m from the BS, n [-] the path loss exponent, and d_{BSi}^{L} [m] the distance between base station BSi and location L (see Section IV-A).

If N_{BS}=2, only locations along the line formed by the two BSs that receive the strongest signals are considered here. If N_{BS}=3, signals from three BSs are considered and the best match on a 2D-grid is considered. The corresponding algorithms for N_{BS}=2 and 3 will be respectively denoted as map_match_2 and map_match_3 hereafter. Fig. 5 (left) illustrates the map matching approach, where BS1 and BS2 are the base stations with the strongest ESP observations. The map_match_2 approach searches the receiver location that has the lowest cost value (eq. (1)) of all points along the line formed by BS1 and BS2 (dark points in left figure), while the map_match_3 approach accounts for all locations in the receiver plane (lighter points in left figure). For these simulations a grid resolution of 10 m is used.

Fig. 5. Candidate node locations according to map_match_2 (dark dots) and map_match_3 (light dots) algorithms (left), and $map\_match\_cent_2$ (dark dots) and $map\_match\_cent_3$ (light dots) algorithms (right).

RSS or ESP values (in dB) do not exhibit a linear relationship with the distance between node and BS, but instead,

they have an exponentially decreasing relationship, so that one-slope log-distance models are often used. As a consequence, given that RSS values are traditionally homoscedastically distributed across all distance values, errors on the distance estimation become larger for lower RSS values and thus, for larger distances. As such, RSS-based location accuracy is typically worse in outdoor environments, due to (i) the large distances between the mobile nodes and the BSs and (ii) the relatively large variances of the shadowing fading around the path loss model in case of Non-Line-of-Sight situations.

5) RSS centroid map matching: The RSS centroid map matching algorithm follows the same approach as the map matching algorithm from the previous section. However, while the map matching algorithm considers *all* locations along a (theoretically infinite) line (for N_{BS}=2) or plane (for N_{BS}=3), the RSS centroid map matching algorithm limits the set of candidate locations to the *line segment* between the two BSs (for N_{BS}=2), and to locations within the *triangle* formed by the three BSs (for N_{BS}=3). These algorithms will be denoted as $map\_match\_cent_2$ and $map\_match\_cent_3$, respectively. Fig. 5 (right) illustrates the centroid map matching approach. For the simulations a grid resolution of 10 m is used.

B. Road mapping filter

All of aforementioned localization algorithms will deliver a set of raw location estimates (see Fig. 4). By inputting these estimates to a road mapping filter, the estimation accuracy of these temporary estimates can be improved by mapping the estimated position onto a road segment (by assuming the node is located on a road). Another improvement is possible by accounting for the maximal node velocity. For example, when moving at a maximal speed of 2 m/s, we know that after 30 seconds the next update should be within 60 m of the previous location update. As such, the more raw location estimates per time unit, and the lower the maximal node velocity, the more improvement can be expected from the road mapping filter. By taking into account consecutive raw location estimates, the road infrastructure layout and the allowed speed limits, we can improve the prediction by calculating the most likely path in a certain time span. This additional road mapping filter ensures realistic and actually possible trajectories.

First, in an offline phase, the road infrastructure layout is converted to a grid of possible positions by making use of OpenStreetMap data. All major and minor roads are divided in pieces of 20 m and all grid points along the road segments keep a link to their neighboring grid points. In the online phase, the first raw location estimate serves as starting point, initialized with a cost of zero. In total, the 1000 points that are the closest to this starting point and that are located on a route, are retained as well, using a grid spacing of 50 m. Retaining these 1000 points for further calculation increaeses robustness against a bad starting point estimation. Next, when a new raw location estimate is available, all reachable grid points seen from these starting points are calculated by recursively making use of the neighboring grid points, speed limits, and time passed between this and the last raw estimate update. These reachable grid points make up the end points of the new paths and retain a cost and link to the previous point (i.e., parent grid point). The cost of each path is updated as the cost of the previous point added with the distance between this point and the raw location estimate. In the next iteration, the end points of all paths in memory are updated again with this technique. To limit memory usage, the filtering algorithm only retains the 1000 most likely paths at each time instance. At the end of the time span, all parent grid points from the path with the current lowest cost are looked up in memory and form the final predicted trajectory for this user. For more info about this approach, we refer to [13]. The outcome of the road mapping filter is a more precise trajectory estimation. All that is needed for the algorithm is map info and the speed limits along each road segment, provided by OpenStreetMap data. Here, we assume that the mobility profile is known a priori: a maximal speed of 5 km/h and 25 km/h is assumed for the walking and cycling route, respectively. The maximal speed for the driving route is limited to the allowed speed on that road segment.

In this paper, four data sets of raw location outputs will be inputted into the road mapping filter, as shown in Fig. 4.

- Two data sets used for comparing the effect of the road mapping filter on different RSS-based raw location estimates. This filter can be applied to all measured samples, irrespective of the number of BSs that have received the signal (N_{BS}= 1, 2, or 3), as even for only one received sample, a raw location estimate can be calculated via the $proximity$ algorithm.
  - $proximity$-$centroid_2$-$centroid_3$ (also denoted as $prox - cent$): if one BS receives a signal, the $proximity$ estimate is used as input for the road mapping filter, the $centroid_2$ algorithm for N_{BS}=2, and $centroid_3$ for N_{BS}= 3. This raw location set can be easily obtained without any advanced processing.
  - $proximity$-$map\_match\_cent_2$-$map\_match\_cent_3$ (also denoted as $prox - mmc$): if one BS receives a signal, the $proximity$ estimate is used as input for the road mapping filter, the $map\_match\_cent_2$ algorithm for N_{BS}= 2, and $map\_match\_cent_3$ for N_{BS}= 3. This raw location set requires some processing and knowledge of the propagation in the environment, but is expected to be more accurate.
- Two data sets for comparing the effect of the road mapping filter on TDoA and RSS estimates. Since the $tdoa$ algorithm can only be applied to samples that are collected at three BSs, we will here only evaluate the location accuracy for samples where N_{BS}=3, in order to guarantee a fair comparison between RSS and TDoA performance. However, all other raw RSS location outputs (collected at only 1 or 2 BSs) can also be used as input to the road mapping filter, as these estimates are available and are a useful input to the road mapping filter.
  - $proximity$-$map\_match\_cent_2$-$map\_match\_cent_3$ (also denoted as $prox - mmc(3)$): same dataset as

defined above, but only evaluated at samples where N_{BS}= 3.
- $tdoa$: the location estimates of the $tdoa$ algorithm are used as input for the road mapping filter.

IV. Results

A. ESP model

Table III shows the characteristics of the one-slope models that link the estimated signal power ESP for each of the three scenarios to the distance between mobile node and BS. These models were obtained by least-square fitting. The table shows that no large differences are observed between 'walking', 'cycling', and 'driving', with mainly a slightly lower ESP in the 'driving' scenario, probably due to the vehicle penetration loss (n slightly higher for 'driving'). These models will be used in eq. (1) for the map_match and map_match_cent algorithms.

TABLE III
ESP one-slope model characteristics for the three scenarios.

scenario	ESP_{100} (dB)	n (-)	σ (dB)
walking	-90.64	1.96	7.16
cycling	-87.06	1.99	7.89
driving	-90.78	2.03	7.29

B. Raw location estimates

1) RSS-based algorithms: Measurement samples either yield measurements from 1, 2, or 3 BSs (N_{BS}= 1, 2, or 3). Certain algorithms are suitable for all sample types (e.g., $proximity$), others require measurements at 3 BSs (e.g., $centroid_3$), see Fig. 4. Therefore, the results will differentiate between measurements that contain 1, 2, and 3 BS reports respectively, in order to consider the same dataset for each localization technique and obtain a fair comparison.

Table IV lists the number of samples N_S per dataset, and the median (p_{50}) and maximal (p_{95}) errors per localization technique, cumulated over all SFs. For the walking scenario, the (four) $centroid$ and map_match_cent algorithms deliver comparable results for samples with 3 BS observations with a p_{50} between 2339 m ($centroid_2$) and 2482 m ($map\_match\_cent_2$), and a p_{95} between 5576 m ($centroid_3$) and 6954 m ($centroid_2$). When considering all three scenarios, $map\_match\_cent_3$ performs slightly better than these other three algorithms, and $map\_match\_cent_2$ outperforms $centroid_2$, at the expense of additional processing. E.g., for N_{BS}= 3, the average of the median errors over the three scenarios is 1817, 1885, 1902, and 2061 m for $map\_match\_cent_3$, $map\_match\_cent_2$, $centroid_2$, and $centroid_3$, respectively.

Compared to these four algorithms, the $proximity$ algorithm generally delivers results with a slightly higher error for N_{BS}= 3 (median error of 2356 m on average over the three scenarios for N_{BS}= 3), mainly due to the larger error in the 'walking' and 'driving' scenarios. For $N_{BS} = 2$ however, $proximity$ performs well, especially for 'walking' route (median error of 1670 m). This inconsistency is explained by the fact that the 'walking' and 'cycling' results are very dependent on the specific route. E.g., the 'walking' route covers a smaller area (874 x 707 m) and is located very close to a specific BS. As such, a large set of $proximity$ estimates can be exceptionally good. This is best seen for the samples with only one observation, where the median error is only 734 m. As the 'driving' route covers a much larger area (12631 x 9543 m), the obtained results are more averaged with respect to node vs. BS location, and are therefore more generally valid in the authors' opinion.

A clear trend is that predictions for the 'driving' route are better than for the other scenarios, for all algorithms. The reason is not that the predictive power of the ESP model is better for the 'driving' route (σ around 7 dB for all scenarios in Table III), but that the median distance between the measurement locations and the observing BS is lower for the 'driving' route (2218 m and 2439 m for $N_{BS} = 2$ and $N_{BS} = 3$ respectively) than for the 'walking' (2954 m and 3424 m for $N_{BS} = 2$ and $N_{BS} = 3$ respectively) and 'cycling' (2624 m and 3033 m for $N_{BS} = 2$ and $N_{BS} = 3$ respectively) routes. Since also the number of recorded samples is lower for 'driving', the reason for this lower median distance is probably that, because of vehicle attenuation, mainly the samples are retained where the BSs are relatively close to the mobile node and packet reception is still possible. This effect of this lower node-to-BS distance is not only reflected in the performance of the $proximity$ and $centroid$ algorithms, but also in that of the map_match and map_match_cent algorithms: a one-slope model prediction error of e.g., 7 dB (vs. the measurement) leads to smaller estimation errors at smaller distances than at larger distances, due to the ESP (in dB) being linearly dependent on the *logarithm* of the distance.

Another clear trend is the performance of the (traditional) map_match algorithms. Although they are more advanced than the $proximity$ and $centroid$ algorithms, their median error is similar or larger than these algorithms in all three scenarios ('walking', 'cycling', 'driving'), and the maximal error is larger in each case. This can again be explained by the fact that a measured ESP value that is lower than is expected based on the model, can significantly pull away the location estimate from the real location. This behaviour is particularly noticed in the high maximal errors for the map_match algorithms. E.g., if for a location at 2500 m from a BS in the walking scenario, the measured ESP is 5 dB lower than estimated by the model (e.g., due to shadowing), the estimated distance is 4504 m, corresponding to an error of 2004 m. As shown earlier, the map_match_cent approaches efficiently tackle these problems, with a significantly improved performance.

It should be noted that the map_match and map_match_cent algorithms in their current form use ESP models that are a best one-slope fit to the collected measurements. Besides requiring a training phase prior to deployment, this model is also the best possible (one-slope) model for this data set. A slightly worse behavior is expected when a more generic propagation

TABLE IV

MEDIAN (p_{50}) AND MAXIMAL (p_{95}) POSITIONING ERROR OF RAW LOCATION ESTIMATES FOR 'WALKING', 'CYCLING', AND 'DRIVING', ACCORDING TO THE ALGORITHMS DESCRIBED IN SECTION III-A, WITH A DISTINCTION BETWEEN SAMPLES BEING OBSERVED BY A DIFFERENT NUMBER OF BSS (N_{BS} = 1, 2, 3). N_S IS THE NUMBER OF COLLECTED SAMPLES PER CASE. THE CONSIDERED DATA SET COMPRISES ALL SIX SFS (SF7-SF12).

N_{BS} (-)	Algorithm	**walking**			**cycling**			**driving**		
		N_S (-)	p_{50} (m)	p_{95} (m)	N_S (-)	p_{50} (m)	p_{95} (m)	N_S (-)	p_{50} (m)	p_{95} (m)
1	$proximity$	900	734	5186	748	1262	3687	704	1455	3317
2	$proximity$	218	1670	7320	166	2017	6265	188	1708	4778
	$centroid_2$		2657	4879		1867	5724		1420	4153
	map_match_2		2403	11964		2874	11864		1569	8331
	$map\_match\_cent_2$		1346	4820		1664	4656		1137	3335
3	$proximity$	414	3202	6233	425	2145	5985	202	1722	3733
	$centroid_2$		2339	6954		1931	5609		1437	4207
	$centroid_3$		2392	5576		2270	5265		1522	3922
	map_match_2		3674	8708		2269	8551		1334	5817
	$map\_match\_cent_2$		2482	6499		1888	5051		1284	3454
	map_match_3		3681	7320		2507	7399		1589	6788
	$map\_match\_cent_3$		2347	6018		1864	5174		1239	3453
3	$tdoa$	341	207	578	348	222	592	77	145	506

TABLE V

MEDIAN (p_{50}) AND MAXIMAL (p_{95}) POSITIONING ERROR FOR THE DIFFERENT ALGORITHMS, FOR DIFFERENT SFS, WITH A DISTINCTION BETWEEN SAMPLES BEING OBSERVED BY A DIFFERENT NUMBER OF BSS (N_{BS} = 1, 2, 3). N_S IS THE NUMBER OF COLLECTED SAMPLES PER CASE. ($prox = proximity, cent_i = centroid_i, mmc_i = map\_match\_cent_i$).

'driving'		$N_{BS}=1$	$N_{BS}=2$			$N_{BS}=3$					
		$prox$	$prox$	$cent_2$	mmc_2	$prox$	$cent_2$	$cent_3$	mmc_2	mmc_3	$tdoa$
SF7	N_S (-)	355	84			67					18
	p_{50} (m)	1393	1459	1267	1070	1535	1399	1510	1262	1222	108
	p_{95} (m)	3217	3363	3142	3016	3715	3337	3380	3018	2758	391
SF8	N_S (-)	156	50			63					21
	p_{50} (m)	1455	1819	1488	1285	1617	1252	1489	1198	1186	117
	p_{95} (m)	3592	4741	4588	3335	3450	4097	4119	3515	3520	421
SF9	N_S (-)	102	26			28					13
	p_{50} (m)	1498	1574	1904	1176	1722	1222	1410	1234	1239	192
	p_{95} (m)	3132	5359	4638	3510	6720	4786	4131	4730	3543	432
SF10	N_S (-)	53	14			20					9
	p_{50} (m)	1472	2403	1809	1580	1846	2125	1979	1878	1487	233
	p_{95} (m)	4081	5612	4638	4306	3156	6362	4221	4200	4331	547
SF11	N_S (-)	27	8			16					12
	p_{50} (m)	1930	1651	1619	1188	1585	1705	1129	1401	1196	240
	p_{95} (m)	4425	3101	5278	2082	3421	3130	3015	2856	3732	691
SF12	N_S (-)	11	6			8					4
	p_{50} (m)	2100	1757	1060	887	2184	2294	1868	979	1077	109
	p_{95} (m)	5545	10274	3379	4159	6049	3981	5362	3981	3532	195

model would be used.

2) TDoA-based algorithm: The $tdoa$ algorithm performance is significantly better than the RSS-based algorithms, with median errors p_{50} between 145 m ('driving') and 222 m ('cycling'), and maximal errors p_{95} between 506 m ('driving') and 592 m ('cycling'). Although the positioning accuracy clearly outperforms that of any RSS-based algorithm (see previous section), location updates are much less frequent. For the walking and cycling scenarios, the ratio of TDoA samples and RSS samples (i.e., all samples) is 22% and 26%, respectively, meaning that for approximately each four RSS-based location estimates, only one TDoA-based location estimate is obtained (cumulated over all SFs). For the 'driving' scenario, this ratio drops to only 7%. In practice, one should expect that the number of location updates for $tdoa$ (e.g., 341 for 'walking') would be equal to the number of RSS updates when $N_{BS} = 3$ (e.g., 414 for 'walking'). However, some of the BS were not equipped with GPS and could therefore not be used for a TDoA calculation. In the city centre, where the 'walking' and 'cycling' routes were traveled, relatively more BS were GPS-equipped, leading to a better match of the N_S values compared to the 'driving' scenario. It also has to be noted that this number of samples is cumulated over all SFs, while in reality only one SF will be used. It was shown in [8] that there was no consistent trend in TDoA localisation accuracy with respect to the SF, so the SF providing the largest amount of updates could be considered as the optimal SF. In the next section, the impact of the SF on RSS- and TDoA-based localisation will be further detailed.

3) Impact of spreading factor: In [8], it was shown that no consistent relation was observed between the SF and the positioning accuracy for the $tdoa$ algorithm. Therefore, the SF delivering the most location updates per unit of time could be considered as optimal. For this test, SF8 delivered the

best tradeoff between a small transmission interval (preferring a low SF) and a sufficient range to reach 3 BS and be able to perform a TDoA location estimate (preferring a high SF). Table V, showing the median (p_{50}) and maximal (p_{95}) positioning errors for the 'driving' scenario for the different algorithms, confirms this: the most location updates for TDoA (21 updates) are obtained for SF8. Similar conclusions were obtained for the 'walking' and 'cycling' scenarios in [8].
In the following, the impact of the spreading factor on RSS-based location estimates will be assessed for the 'driving' scenario, as this scenario is the least trajectory-dependent, thanks to the larger area that is considered.

a) Number of RSS location updates per SF: Table V shows N_S, the number of measurement samples per N_{BS} and per SF. For the driving scenario, the number of RSS updates (e.g., 355 + 84 + 67 = 506 for SF7) is much larger than the number of TDoA updates (e.g., 18 for SF7). A similar observation is made for the other SFs. As can be expected, the number of updates is much higher for lower SFs, as the minimal transmission interval is shorter [8]: the total number of RSS updates drops from 506 for SF7 to 269 for SF8 and to 25 for SF12. Unless the positioning accuracy is better for higher SFs, this shows that the lowest SF (i.e., SF7) is preferable to perform RSS-based location tracking.

b) RSS positioning accuracy per SF: It was observed that for higher SF, the fraction of measurement samples containing 3 BS observations ($N_{BS} = 3$) increases, while the number of samples containing only one observation ($N_{BS} = 1$) increases. E.g., for the 'walking' scenario, 71% of the samples are $N_{BS} = 1$ and 18% are $N_{BS} = 3$, while for SF12, 18% are $N_{BS} = 1$ and 55% are $N_{BS} = 3$. Indeed, because of the larger range for SF12, the fraction of reports with 3 BS observations increases with the SF. However, as was shown in Table IV, no overall significant positioning improvement was noticed when more BSs observe a signal (i.e., $N_{BS} = 3$ vs. $N_{BS} = 1$). This is confirmed in Table V: no consistent trend is noticed when the SF changes. As the accuracy conclusions for each algorithm are also applicable per SF, only a limited subset of RSS algorithms is considered in Table V. The $proximity$ algorithm seems to be an exception: the performance of this algorithm slightly decreases with SF (for all N_{BS} values). Since larger SFs have a larger range, there is an increased chance that a more distant BS will record the strongest ESP, while no measurement report might have been obtained in the same case for a lower SF, meaning that lower SFs have a larger chance of recording an observation of a more nearby BS. This increasing error is also noticed in the p_{95} values. It can be concluded that no significant difference in accuracy is observed between SFs, neither for TDoA or for (the best performing) RSS-based algorithms. Hence, the optimal choice is the SF yielding the largest number of location updates per time unit, i.e., SF7.

C. Effect of road mapping filter on raw location estimates

This section will assess the effect of applying a road mapping filter (see Section III-B) to the raw location estimates. It was shown that SF8 was the best choice for $TDoA$, whereas for RSS-based positioning, SF7 is preferred. SFs higher than 8 will therefore not be investigated here, since (1) less benefit is obtained from the road mapping filter when a lower number of location updates per time unit is provided and (2) the previous section did not indicate that raw location updates are more accurate when the SFs increases. Table VI shows the positioning accuracies after applying a road mapping filter to the raw RSS and TDoA estimates, for SF7 and SF8. For RSS, the datasets described in Section III-B and shown in Fig. 4 are used ($prox - cent$ and $prox - mmc$).

1) Performance of road mapping filter for SF7: Table VI shows that the road mapping filter successfully decreases the median positioning errors. For 'walking', the already low median errors (around 830 m) are further decreased to around 650 m. The algorithm particularly succeeds in limiting the maximal errors (from more than 4000 m for SF7, to less than 1000 m). For the 'driving' scenario, median errors decrease by around 50%, from around 1400 m to around 700 m. Maximal errors decrease from around 3000 m to around 2000 m.

2) Comparison of RSS algorithms after application of road mapping filter for SF7: Although the $prox - mmc$ approach requires a prior characterization of the propagation environment and a more advanced processing than $prox - cent$, its performance is not significantly better (e.g., p_{50} of 706 m vs. 724 m for 'driving'). In some cases, the $prox - cent$ approach even performs better (e.g., maximal errors are lower for 'walking' and 'cycling').

3) Comparison of RSS and TDoA for SF7: It is observed that the road mapping filter only succeeds in improving performance for $tdoa$ for the lowest mobility profile ('walking'). $tdoa$ median and maximal errors are in the order of 100-200 m and 300-400 m respectively. Although the road mapping filter significantly improves RSS-based localization ($prox - mmc(3)$), the performance is still not comparable to the $tdoa$ performance, although median errors below 400 m are obtained for the 'driving' scenario. Maximal errors vary between 1075 m ('walking') and 1980 m ('cycling'). However, the number of location updates per time unit using SF7 is around 10 times higher for RSS algorithms than for the TDoA algorithm (partly due to the fact that not all LoRa BS are GPS-equipped, see Section IV-B2).

4) Impact of spreading factor - SF8 vs. SF7: Although it was expected that the performance of the RSS algorithms at SF7 after applying the filter would outperform the performance at SF8, the difference is very limited. E.g., for $prox - mcc$ and for both SFs, median accuracies are around 600-700 m for the 'walking' scenario, and around 900 m and 700 m for the 'cycling' and 'driving' scenarios, respectively. It appears that the number of updates at SF8 is still sufficient to benefit from the mapping algorithm. It can be noticed that, unlike for SF7, the road mapping filter better succeeds in improving the accuracy for $tdoa$, with a median error of only 86 m for the driving scenario.

TABLE VI
MEDIAN (p_{50}) AND MAXIMAL (p_{95}) POSITIONING ERROR FOR THE DATASET DESCRIBED IN SECTION III-B FOR SF7 AN SF8, WITH AND WITHOUT ROAD MAPPING FILTER DESCRIBED IN SECTION III-B.

	SF7				**SF8**			
'walking'	without filter		with filter		without filter		with filter	
	p_{50} (m)	p_{95} (m)	p_{50} (m)	p_{95} (m)	p_{50} (m)	p_{95} (m)	p_{50} (m)	p_{95} (m)
$prox-cent$	830	4105	631	916	1587	5580	660	1334
$prox-mmc$	837	4268	669	928	960	5601	598	933
$prox-mmc(3)$	2189	5843	716	1075	2388	5244	584	990
$tdoa$	221	566	118	309	194	696	98	351
'cycling'	without filter		with filter		without filter		with filter	
	p_{50}	p_{95}	p_{50}	p_{95}	p_{50}	p_{95}	p_{50}	p_{95}
$prox-cent$	1392	4588	943	1595	1840	5432	1009	2439
$prox-mmc$	1323	3812	879	1821	1646	5462	917	2051
$prox-mmc(3)$	1891	4246	918	1980	1911	5786	875	1981
$tdoa$	192	583	192	407	249	681	183	416
'driving'	without filter		with filter		without filter		with filter	
	p_{50}	p_{95}	p_{50}	p_{95}	p_{50}	p_{95}	p_{50}	p_{95}
$prox-cent$	1403	3253	724	2039	1462	4012	701	1851
$prox-mmc$	1305	3067	706	2039	1382	3528	704	1925
$prox-mmc(3)$	1267	2941	371	1402	1176	3591	495	1302
$tdoa$	108	391	109	429	117	421	86	342

V. CONCLUSION

This paper presented a performance comparison of RSS-based and TDoA-based localisation approaches in a public outdoor LoRa network. For the considered network in the Netherlands, raw location estimates of TDoA approaches outperform all investigated RSS approaches, with median errors in the order of 200 m vs. median errors in the order of 1250-2500 m. Except for the simple proximity algorithm, no significant difference in positioning accuracy is observed for different spreading factors. For RSS-based algorithms, the largest number of location updates per time unit is possible for SF7, whereas for the TDoA algorithm, the optimal spreading factor is SF8. Application of a road mapping filter on raw RSS-based location estimates yields a median error of around 700 m for a car trajectory, an improvement of 50%. Maximal errors can be limited to around 2 km. It is shown that simple RSS approaches using proximity and centroid techniques achieve comparable accuracies as more advanced RSS algorithms, mainly due to quite large shadowing fading values. Future work consists of investigating more routes to obtain more representative results and make general conclusions. Also combined TDoA and Angle-of-Arrival-approaches will be investigated.

ACKNOWLEDGMENT

This work was executed within HYCOWARE, a research project bringing together academic researchers and industry partners. The HYCOWARE project was co-financed by imec (iMinds) and received project support from Flanders Innovation & Entrepreneurship.

REFERENCES

[1] D. F. Carvalho, A. Depari, P. Ferrari, A. Flammini, S. Rinaldi, and E. Sisinni, "On the feasibility of mobile sensing and tracking applications based on lpwan," in *2018 IEEE Sensors Applications Symposium (SAS)*, March 2018, pp. 1–6.

[2] M. Mirza, Y. A. Ahmad, and T. S. Gunawan, "Low altitude balloon iot tracker," in *2017 IEEE 4th International Conference on Smart Instrumentation, Measurement and Application (ICSIMA)*, Nov 2017, pp. 1–6.

[3] M. S. Tanaka, Y. Miyanishi, M. Toyota, T. Murakami, R. Hirazakura, and T. Itou, "A study of bus location system using lora: Bus location system for community bus "notty"," in *2017 IEEE 6th Global Conference on Consumer Electronics (GCCE)*, Oct 2017, pp. 1–4.

[4] J. G. James and S. Nair, "Efficient, real-time tracking of public transport, using lorawan and rf transceivers," in *TENCON 2017 - 2017 IEEE Region 10 Conference*, Nov 2017, pp. 2258–2261.

[5] T. Hadwen, V. Smallbon, Q. Zhang, and M. D'Souza, "Energy efficient lora gps tracker for dementia patients," in *2017 39th Annual International Conference of the IEEE Engineering in Medicine and Biology Society (EMBC)*, July 2017, pp. 771–774.

[6] A. M. Baharudin and W. Yan, "Long-range wireless sensor networks for geo-location tracking: Design and evaluation," in *2016 International Electronics Symposium (IES)*, Sept 2016, pp. 76–80.

[7] B. C. Fargas and M. N. Petersen, "Gps-free geolocation using lora in low-power wans," in *2017 Global Internet of Things Summit (GIoTS)*, June 2017, pp. 1–6.

[8] N. Podevijn, D. Plets, J. Trogh, L. Martens, P. Suanet, K. Hendrikse, and W. Joseph, "TDoA-based Outdoor Positioning with Tracking Algorithm in a Public LoRa Network," *Wireless Communications and Mobile Computing*, in press.

[9] K. H. Lam, C. C. Cheung, and W. C. Lee, "Lora-based localization systems for noisy outdoor environment," in *2017 IEEE 13th International Conference on Wireless and Mobile Computing, Networking and Communications (WiMob)*, Oct 2017, pp. 278–284.

[10] H. Sallouha, A. Chiumento, and S. Pollin, "Localization in long-range ultra narrow band iot networks using rssi," in *2017 IEEE International Conference on Communications (ICC)*, May 2017, pp. 1–6.

[11] R. Kaune, "Accuracy studies for tdoa and toa localization," in *2012 15th International Conference on Information Fusion*, July 2012, pp. 408–415.

[12] D. Plets, W. Joseph, E. Tanghe, L. Verloock, and L. Martens, "Analysis of propagation of actual dvb-h signal in a suburban environment," in *2007 IEEE International Symposium on Antennas and Propagation*, Honolulu, Hawaii, USA, 10 - 15 June 2007, pp. 1997 – 2000, paper No. 1386.

[13] J. Trogh, D. Plets, L. Martens, and W. Joseph, "Advanced real-time indoor tracking based on the viterbi algorithm and semantic data," *International Journal of Distributed Sensor Networks*, vol. 11, no. 10, 2015. [Online]. Available: http://dsn.sagepub.com/content/11/10/271818.abstract